THE ASTROPHYSICAL JOURNAL, 279:567–577, 1984 April 15

THE POPULATION STRUCTURE OF THE WING OF THE SMALL MAGELLANIC CLOUD

EDUARDO HARDY[1] AND DANIEL DURAND
Département de Physique and Observatoire du Mont Mégantic, Université Laval, Québec
Received 1983 July 25; accepted 1983 October 4

ABSTRACT

Deep and rich color-magnitude diagrams are presented for four field areas in the Wing of the Small Magellanic Cloud (SMC) near the clusters NGC 376, NGC 416, and NGC 419. The interpretation of the diagrams in terms of preponderant epochs of star formation is shown to depend critically on the distance and reddening scales adopted for the SMC. Under our preferred scales the presence of a well-populated subgiant branch indicates the existence of an underlying intermediate-age population which is older than 3 Gyr and which may be proportionally more important in the SMC field than in the field of the Large Magellanic Cloud. It would seem that although stars of all ages are probably present in both Clouds, the median age of star formation is older in the SMC field.

Subject headings: galaxies: Magellanic Clouds — galaxies: stellar content — stars: evolution

I. INTRODUCTION

The purpose of this paper is to present and interpret color-magnitude (*C-M*) diagrams of Small Magellanic Cloud (SMC) fields in the general region known as the "Wing" of the Cloud, which corresponds to the SMC eastern extension toward the Large Cloud. The ultimate goal of this type of investigation involving classical techniques such as the construction of *C-M* diagrams is that of establishing the history of star formation and chemical evolution in the few galaxies which are sufficiently nearby that individual field stars can be resolved and measured.

Most of the information concerning stellar populations in the Magellanic Clouds pertains to their rich system of clusters (see Hodge 1982 for a review). Recently, however, a number of studies have been undertaken in areas of the Clouds, particularly in the Large Magellanic Cloud (LMC) (Stryker and Butcher 1981; Hardy *et al.* 1984) with the aim of determining a main sequence (MS) luminosity function and establishing preponderant ages of star formation. In the recent past use of electronographic cameras (i.e., Walker 1972) has provided faint stellar sequences, mainly around populous clusters, but because of the restricted area covered (a characteristic shared by the new generation of solid-state devices) the statistics on sequences in the *C-M* diagram are somewhat poor. An alternative approach, which is the one used in this investigation, is to make use of large-scale photographic plates calibrated via the electronographic sequences to generate very well populated *C-M* diagrams to moderately faint magnitudes. This approach yields statistically well-defined sequences which then can be compared with evolutionary models and with observations of different regions.

Some information exists on the field population of the SMC, and most of it has been derived as a by-product of the study of rich clusters (but see Brück and Marsoglu 1978). We have chosen to study the SMC Wing for the following reasons: (1) It contains some of the brightest and richest clusters in the SMC: NGC 419, NGC 416, and NGC 376, of which only NGC 419 has been previously studied (Arp 1958*a*; Walker 1972), which will then provide the deep magnitude sequence required for a study of the field. The study of the clusters themselves (Durand 1982) will be published elsewhere (Durand, Hardy, and Melnick 1984). (2) The SMC Wing links the main body of the SMC to the distorted H I tidal structure known as the Magellanic Stream (Mathewson *et al.* 1979) for which it is not certain that a stellar counterpart has been found so far. (3) The stellar density in the Wing appears to be moderate when compared with the main body of the SMC (Brück 1978), a fact which alleviates the serious contamination problems underlying the construction of faint *C-M* diagrams in the Magellanic Clouds. The general area of the Wing studied here is displayed in *V* and *B* light in Figures 1 and 2. A comparison of the two plates shows the increase in stellar density, particularly of the young blue population, as the main body of the SMC is approached toward the NW.

II. THE DATA

a) Observations and Data Analysis

A set of eight limiting exposures on four visual (103a-D + W16) and four blue (103a-O + W2C) plates were obtained with the 2.5 m du Pont telescope at Las Campanas (scale: 10″.9 mm^{-1}) under good seeing conditions. Figures 1 and 2 show the areas studied. These areas were digitized in Geneva with the ESO Optronix microdensitometer using steps of 30 μm, corresponding to 0″.33 per pixel. Table 1 lists the relevant data pertaining to the observed areas. The reduction procedure (Durand 1982) is quite complex and was designed to deal in an automatized way with a very large number of stars while taking into consideration: (1) the presence of crowding, (2) the need to obtain accurate magnitudes inside a large dynamical range of almost 5 mag, and (3) the possibility of using not only the standard stars but all stars in common between plates to perform the final

[1] Guest Investigator, Las Campanas Observatory, Carnegie Institution of Washington.

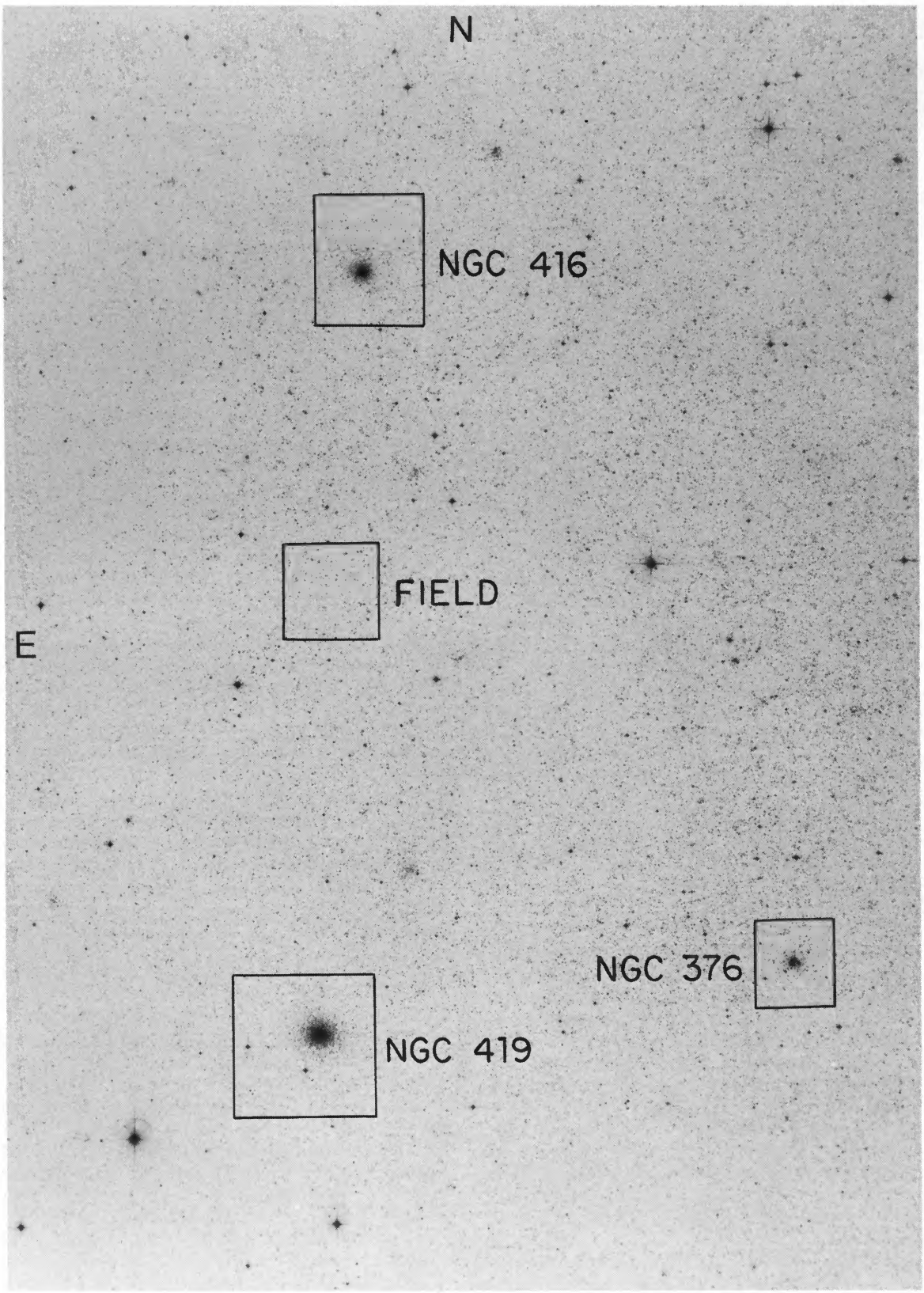

FIG. 1.—A visual limiting exposure with the du Pont 1.5 m telescope of the regions studied in the Wing of the SMC. The side of the square around NGC 419 corresponds to 6′.

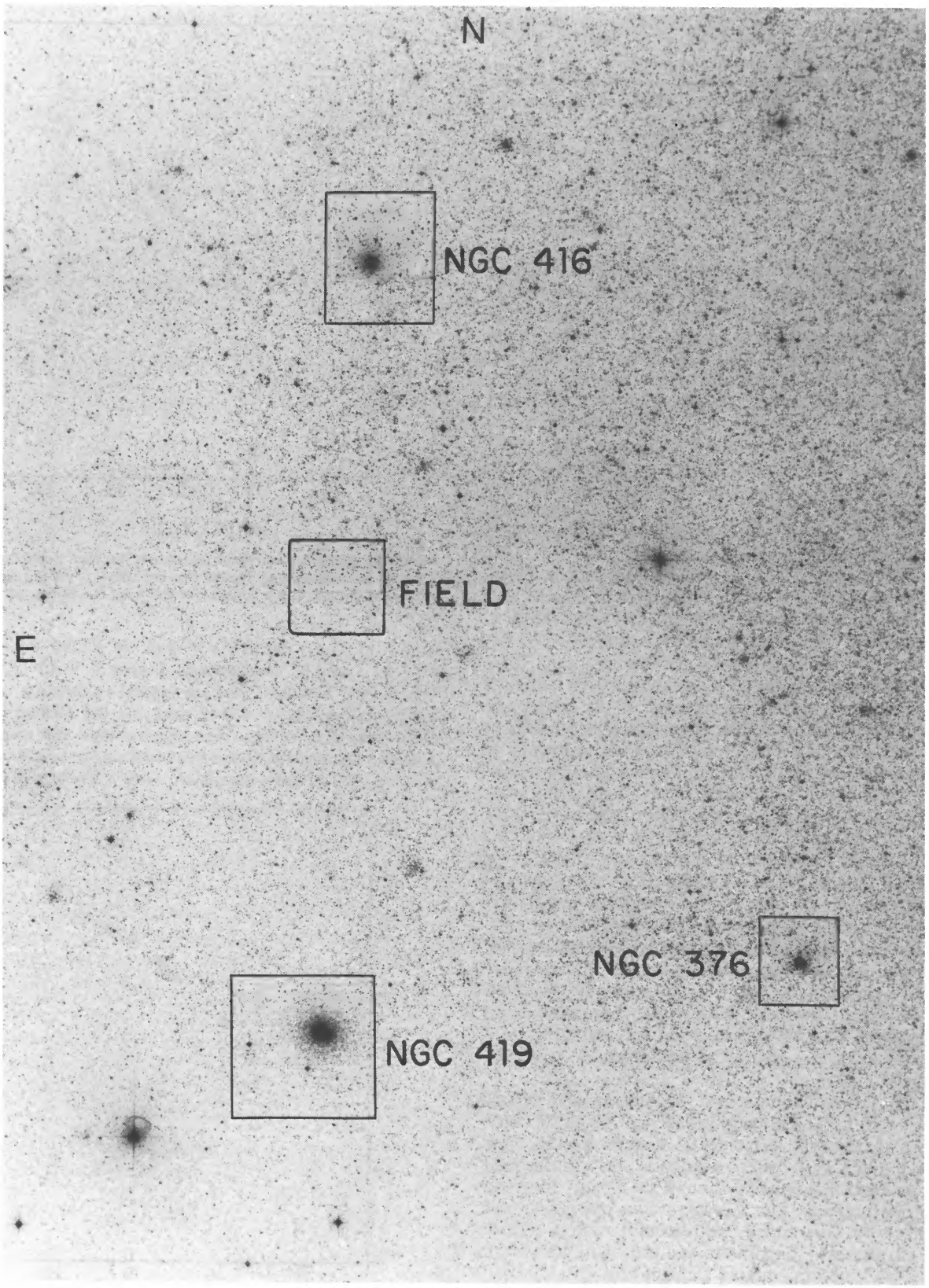

FIG. 2.—Same as Fig. 1 but in the *B* filter. Notice the differences in the distribution of the young blue population and the older and more uniform red underlying population when Figs. 1 and 2 are compared.

TABLE 1

POSITIONS AND EFFECTIVE SURFACES

Region	R.A. (1975)	Decl.	A (sq. arcmin)
NGC 376	$01^h30^m.0$	$-72°57'$	6.5
NGC 416	01 07.4	−72 29	7.0
NGC 419	01 07.7	−73 09	16.2
Field	01 07.6	−72 42	16.0
Combined	...	...	39.2

reduction into magnitudes (Stetson and Harris 1977). The data were transformed into intensity units via calibration-wedge images exposed onto the plates shortly after the actual exposures. The image of the area in NGC 419 containing the stellar calibration sequence (Walker 1972) was displayed on an image monitor and the digital intensity contrast manipulated so as to unmask the degree of stellar contamination of each stellar image. A selection of standard stars was made on this basis, and an automatized algorithm was tested which rejected the contaminated images on the basis of the detection of multiple centers. The same rejection criterion was later used in the "batch" treatment of all the data. A total of 59 stars out of 146 measured by Walker (1972) and Arp (1958*a*) were retained as standards.

Instrumental magnitudes were obtained through a pixel-summation procedure akin to the Σ-method of Newell and O'Neil (Rheault and Hardy 1980) implemented with a circular aperture and with the background determined from an external annulus. After background subtraction, each pixel was weighted by its intensity (i.e., its information content) in what amounted to adding the squares of the intensities. This procedure had been shown in practice to provide a significant increase in internal precision while reducing, at the same time, the contribution of faint contaminating pixels. It destroys, of course, the linearity of the final calibrating relationship, a consideration of little importance in our case since no extrapolation of the instrumental versus standard magnitude diagram was required. Because the precision of the magnitude determination as a function of image size depends critically on the size of the numerical integration aperture, a continuously variable aperture function was established for each plate using the standard stars as a guide. No single *mean* aperture was found to be able to reproduce the internal precision of the variable-aperture method for both the bright and the faint stars. The same final aperture function was, of course, used for standards and program stars alike, this being the fundamental constraint of the method.

Finally, the procedure described by Stetson and Harris (1977) was used to numerically merge all plates in each bandpass on a common instrumental system. Briefly, each star on each plate of a given bandpass was transformed to the instrumental-magnitude system of the "base" plate via Chebyshev interpolation. The average of four plates provides a more precisely determined instrumental system before reduction into standard magnitudes and uses the information contained in all stars in common, and not only the standard stars, to generate the final magnitudes in the Johnson *BV* system. A small color correction, found as part of the procedure, was applied to the data. The resulting calibration

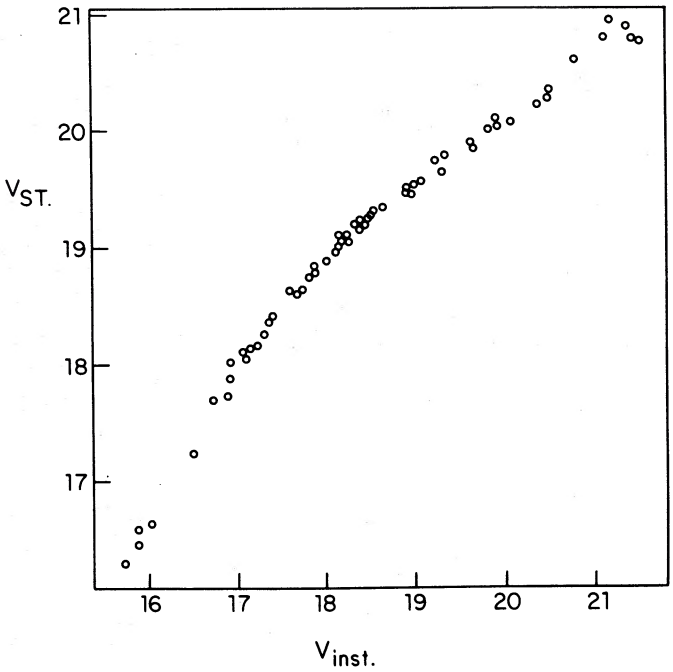

FIG. 3.—The combined calibration curve for four *V* plates (standard vs. instrumental magnitudes). Notice that the curve is not a straight line due to the summation of the squares of the pixel intensities, as described in the text.

curves of the "merged" *V* and *B* plates are shown in Figures 3 and 4, respectively. Figure 4 is to be compared with Figure 5 which shows a typical calibration curve for a single plate giving $\sigma = 0.12$ mag for the fainter half of the standards. The comparison shows that the superposition procedure described above has reduced the scatter by a factor ~ 2 to $\sigma = 0.05$ mag, consistent with a Poissonian process.

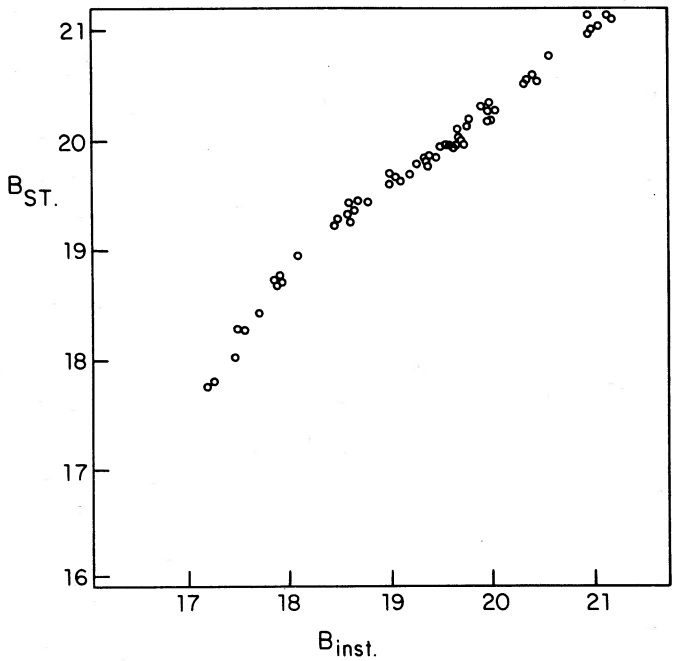

FIG. 4.—Same as Fig. 3 for the four *B* plates.

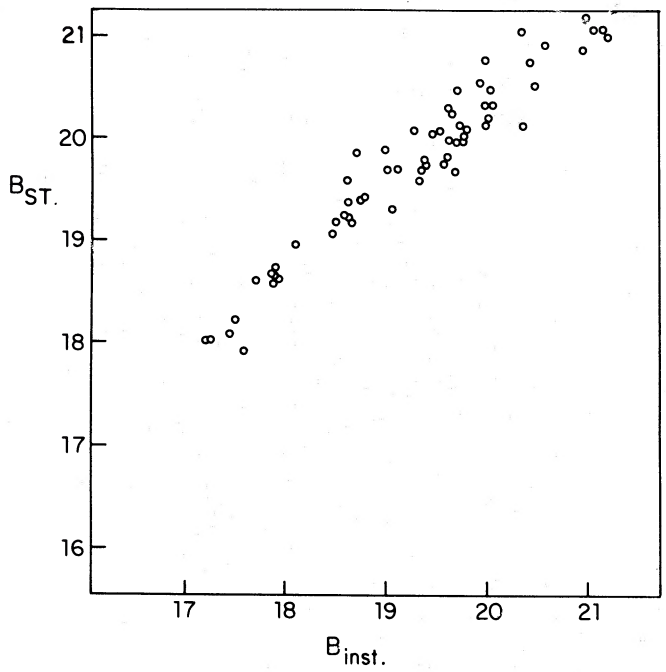

FIG. 5.—A typical calibration curve for a *single* plate. Compare with Fig. 4 to see the improvement introduced by the superposition procedure described in the text.

b) The Color-Magnitude Diagrams

Figures 6, 7, and 8 display the *C-M* diagrams for the areas near NGC 419, NGC 416, and NGC 376, respectively, whereas Figure 9 corresponds to the Field region. The digitized regions are shown in Figures 1 and 2; the areas near the clusters (of surface *A* in Table 1), which belong to the general field, and which are included in the diagrams are those sections of the digitized surfaces which lie well outside the tidal radii of the clusters as determined from stellar counts (Durand 1982; Durand, Hardy, and Melnick 1984). Inspection of the diagrams show that the principal sections of Figures 6, 7, and 9 superpose well on each other. We have therefore generated the combined diagram of Figure 10 so as to increase the number statistics on the different structures. The red giant branch near NGC 376, on the other hand, was found to be systematically shifted toward redder colors and should be considered separately from the rest. Notice that the use of four plates per color will tend to eliminate systematic effects due to spatial plate sensitivity variations or development inhomogeneities, and that observed differences in the diagrams larger than 0.1 mag are very likely real and probably due to reddening, age, and/or metallicity effects. Finally, to provide a further check on the magnitude and color scales we have superposed on Figure 6 the bright reference sequences of Arp and Walker. It is apparent that we have reproduced well the published diagrams while increasing significantly both the size of the sample and the tightness of the sequences.

III. ANALYSIS OF THE FIELD DIAGRAMS

Figure 10 is our fundamental diagram for the study of the SMC Wing. There are three basic features which are useful

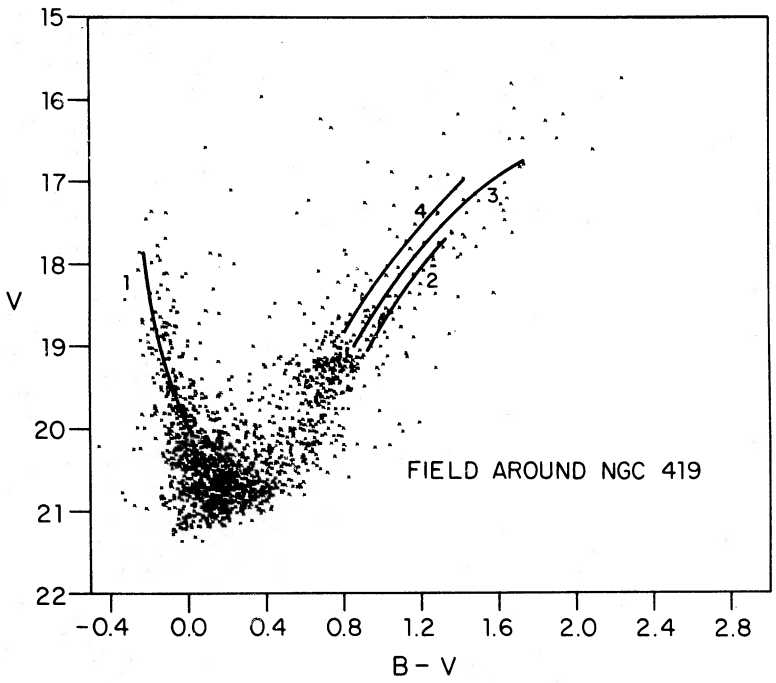

FIG. 6.—The *C-M* diagram for the field around NGC 419. The schematic numbered sequences represent: (1) The main sequence for NGC 419 and NGC 458 (Arp 1958*b*), (2) the red-giant branch for the W side of the SMC (Bruck and Hawkins 1981), (3) Arp's (1958*a*) giant branch for the region near NGC 419, and, (4) the field red-giant branch for the NE outer regions (Bruck and Marsoglu 1978).

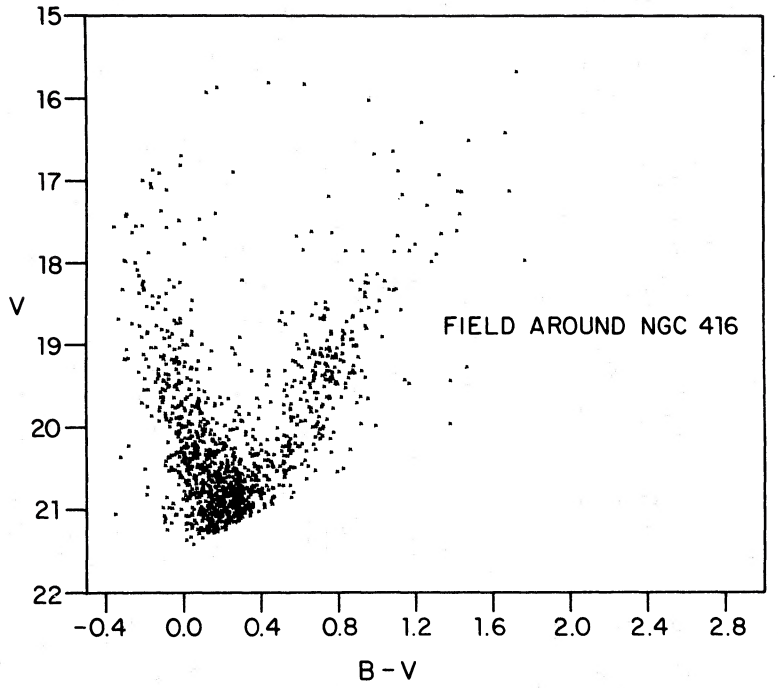

FIG. 7.—The *C-M* diagram for the field around NGC 416

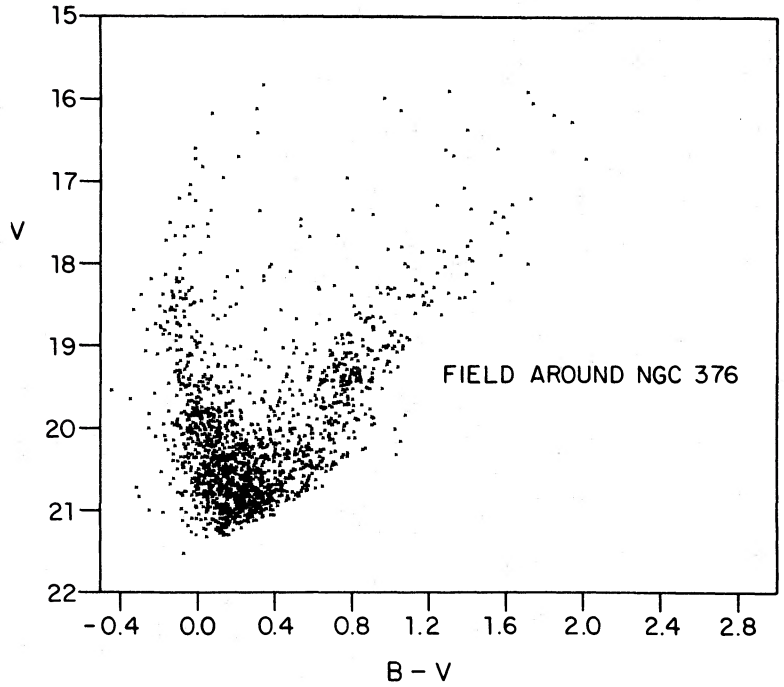

FIG. 8.—The *C-M* diagram for the field around NGC 376

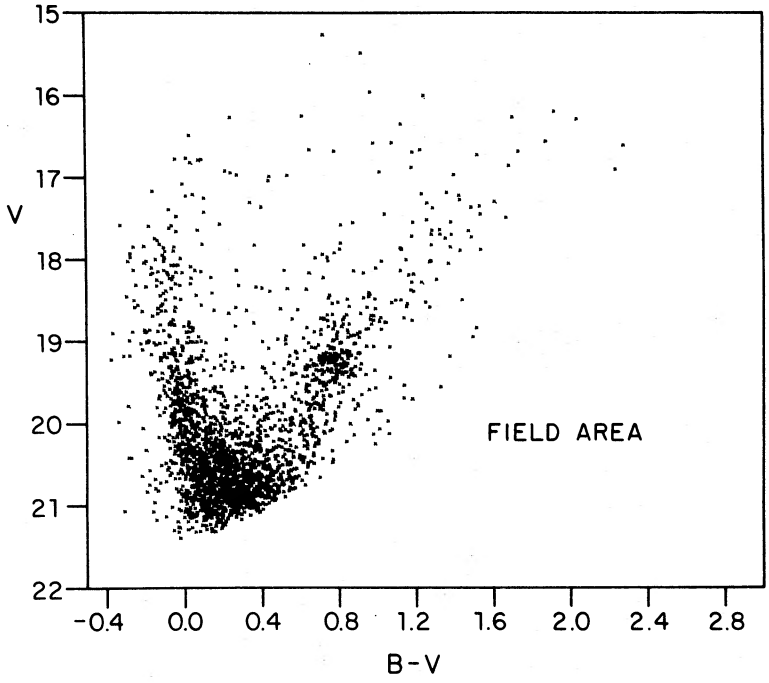

FIG. 9.—The *C-M* diagram for the field region

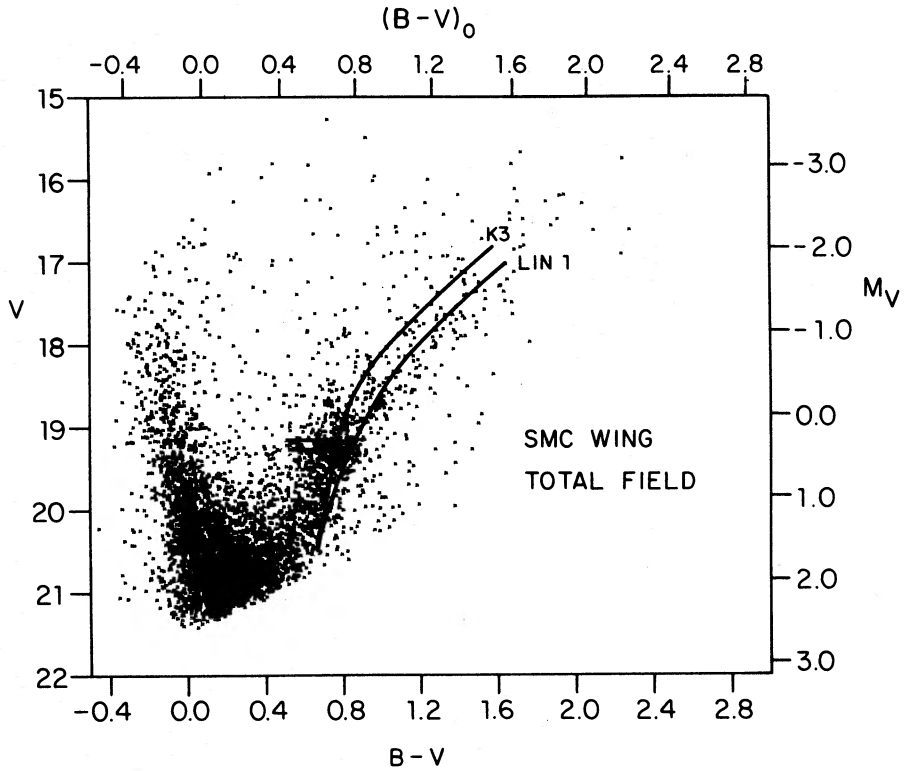

FIG. 10.—The combined *C-M* diagram for all regions except that around NGC 376. The giant and subgiant branches of K3 and L1 (Gascoigne, Bessell, and Norris 1982) are superposed. The levels of their horizontal branches are represented schematically.

TABLE 2

DISTANCE AND REDDENING SCALES

$(m-M)_0$	$(m-M)_{AV}$	A_V	Source
19.27.....	19.33	0.06	Sandage and Tammann 1974 (ST)
18.62.....	18.85	0.23	de Vaucouleurs 1978 (dV)

for our analysis: (1) a well-defined main sequence (MS); (2) a well-populated "clump" at $V \sim 19.3$ and $B-V \approx 0.8$, and (3) a structure located at $V > 19.5$ and $B-V \sim 0.7$ which may be interpreted as a subgiant branch similar to those found in the Galaxy in old Population I clusters such as M67 and NGC 188.

a) The Main Sequence: Distance and Reddening

Prior to any attempted interpretation of Figure 10 in terms of evolutionary sequences or even empirical reference sequences the absolute scales—i.e., distance and reddening—must be established. For the remainder of this paper this problem will be a recurrent one since, as will be shown, the resulting analysis performed under the two current distance scales will lead to quite different interpretations of the stellar content of the SMC. The very cautious comment should be made here that most distance determinations are based on the stellar content of the opposite (i.e., West) side of the SMC. Given the distended nature of the Wing, which links the main body of the SMC to the Magellanic Stream, the possibility of depth effects when comparing both sides of the Cloud should not be completely overlooked.

Table 2 lists the parameters of the two main competing scales. Notice that the difference in absolute distance modulus between the two extreme scales amounts to 0.65 mag, of which 0.23 mag corresponds to differences in the treatment of the extinction. Due to lack of data in the U bandpass we are unable to independently determine the reddening and then to attempt a fundamental determination of the distance from a study of the faint unevolved portion of the main sequence. We can, however, choose between scales on the basis of consistency with the magnitude and colors of the observed main sequence by superposing an appropriate zero-age main sequence which has been corrected for metallicity and evolutionary effects. Figure 11 is a blowup version of Figure 10 over a restricted range of colors. We have superposed there the zero-age main sequence of Mermilliod (1981; his Table 6) for both distance scales after the following abundance correction.

From Patenaude (1978) one has, over the range of interest,

$$M_V = -15\Delta Z + 3\Delta Y \quad (T_e = \text{const}), \tag{1}$$

$$\log T_e = -\Delta Z + 0.15\Delta Y \quad (M_V = \text{const}). \tag{2}$$

For an adopted $Z_\odot = 0.02$ (Hodge 1982) these equations imply a shift of the main sequence toward fainter and bluer magnitudes of $\Delta M_V = 0.24$ and $\Delta(B-V) = 0.03$ if we adopt a value of $[\text{Fe/H}] = -0.70$ ($Z = 0.004$) for the SMC young disk, consistent with the data in Table 4 of Hodge (1982), and leave Y constant. From Figure 11 one sees that the agreement with de Vaucouleurs (1978) (dV) scale is very good. Evolutionary corrections due to the extension toward red colors of the

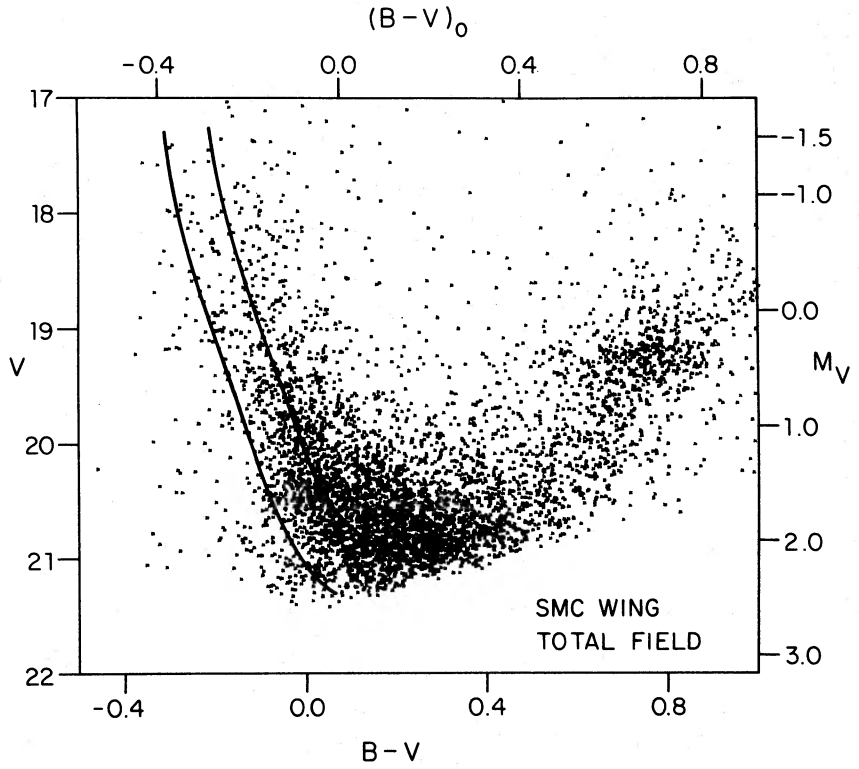

FIG. 11.—A blowup of Fig. 10. The ZAMS, corrected for the metallicity of the SMC, is superposed on the diagram for the two scales of Table 2. The adopted ZAMS (brighter and redder of the two) corresponds to $(m-M)_{AV} = 18.85$.

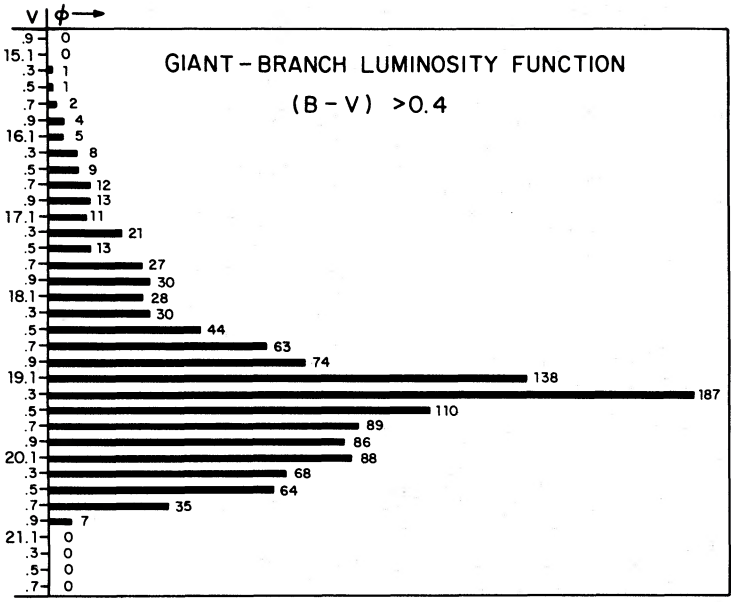

FIG. 12.—The giant-branch luminosity function for all giants with $(B-V) > 0.4$

core hydrogen burning phase can be taken into consideration from the model calculations of Maeder and Mermilliod (1981) by tracing the red envelope of their isochrones (their Figs. 12 and 17) and also from Figure 1 of Mermilliod (1981). This red envelope as applied to the metal-poor zero-age sequence proves also to be consistent with a fit to the short distance. Finally, it should be stressed that the young open clusters NGC 3766, IC 4665, and α Per which have their brightest main-sequence stars at $M_V \sim -3$, as is the case with our main sequence, do join their zero-age main sequence at $M_V \sim 0$ (Mermilliod 1981, Tables 3 and 6). This indicates that we should indeed expect to observe an unevolved main sequence near the faint end of our diagrams. The discrepancies with the long (Sandage and Tammann 1974) distance scale are thus sufficiently important on this side of the SMC that we adopt, within the uncertainties in abundances and reddening, the short distance of Table 2.[2]

b) *The Giant Branch*

The luminosity function corresponding to the giant branch of Figure 10 is shown in Figure 12 in the form of a histogram representing all stars with $B-V > 0.4$. As discussed, the two most conspicuous features are: (1) "clump" visible in Figure 12 as a Gaussian distribution centered at $V = 19.3$ and with a width of ~ 0.4 mag (FWHM); (2) a "subclump" (subgiant branch?) from $V \approx 19.5$, $B-V \approx 0.7$, down to $V \sim 20.5$ and $B-V \sim 0.5$. If we adopt the dV scale instead of that of Sandage and Tammann (1974) (ST), then the giant branch portion of Figure 10 is consistent with a metal-poor version of a group of intermediate-age clusters in the Galaxy characterized by NGC 2420, NGC 2506, and M67 (McClure, Twarog, and Foster 1981). This group appears to set the *lower* age limit (~ 3 Gyr) for the formation of a populated subgiant branch. Notice also (Fig. 10) the morphological similarities with K3 and L1 in the SMC (Gascoigne, Bessell, and Norris 1981).

Demonstrating that the subclump or subgiant structure of Figure 10 is real and not an artifact of the observational errors at faint magnitudes is fundamental for the subsequent analysis. An assessment of the errors involved is thus in order. From the discussion in § II*a* we estimate $\sigma(B-V) \leq 0.10$ mag at the subgiant branch level, although systematic effects in the calibrating sequences amounting to ~ 0.10 mag are probably present (Walker 1972). These errors are not large enough to populate the subgiant locus from the rich main sequence (one would also expect symmetry of residuals with respect to the mean main sequence, which is not the case). Furthermore, the subgiant locus has a well-defined edge on its red side, an edge which is considerably brighter (in B) than the limit of the B plates. Such limit, at $B = 21.5$, defines the diagonal shape of the diagram; the bottom of the subgiant locus lies, on the other hand, almost a full magnitude above the visual plate limit. The above indicates that the subgiant population (whatever its evolutionary interpretation might be) is very likely real, although further and fainter study is clearly called for. The faint intermediate region of the diagram at $(B-V) = 0.3$–0.4 is very likely populated by residuals of faints stars belonging to the main sequence and the subgiant branch.

IV. DISCUSSION AND CONCLUSIONS

The main difficulties in interpreting the *C-M* diagrams of the Wing fields come from the uncertainties in the distance and reddening scales and, to a somewhat lesser degree, in the abundance scale. Not having an independent determination of the reddening, we were forced to choose between the two extreme distance scales on the basis of a main sequence

[2] We have experienced the same difficulties reported here in fitting the *C-M* diagrams of the clusters themselves to the Yale evolutionary sequences when the ST distance (Table 2) and reddening scales were used instead of the dV scales (Durand, Hardy, and Melnick 1984).

fit. The ST distance, even after evolutionary corrections are taken into account, gives a main sequence which is too faint and blue with respect to the observations. If the dV "short" distance is adopted, then the presence of a subgiant branch indicates, by analogy with the Galaxy, that the age of the observed giant branch is older than about 3 Gyr, independently of metallicity (Kinaham and Härm 1975). A small contribution from a globular cluster–like population (i.e., older than 10 Gyr) cannot be excluded, although the observed horizontal branch is morphologically more reminiscent of the "clump" of intermediate-age clusters. This analogy is strenghtened by the similarities between the giant branch of Figure 10 and the *C-M* diagram of K3 (Gascoigne, Bessell, and Norris 1981) for which they give an age of 4 Gyr and a metallicity of [Fe/H] = −0.8. In the Galaxy, NGC 2420 and NGC 2506 show the same global characteristics, although their giant branches are redder, very likely as a result of abundance differences.

The field diagram near NGC 376 (Fig. 8) shows a slight but significant shift toward the red of the giant subgiant branches with respect to the combined diagram of Figure 10. This shift is not present, however, when the main sequences are compared, indicating that age and/or metallicity differences are more likely responsible for it than differential reddening across the face of the SMC. Notice that NGC 376 is closer to the main body of the SMC than the other regions surveyed and, also, that the subgiant branch of Figure 8 provides the best fit to that of L1 for which Gascoigne, Bessell, and Norris (1981) give an age of 8 Gyr.

An increased metallicity or the appropriate variation in the He content (eqs. [1] and [2]) could have decreased the discrepancies between the observed *C-M* diagram and the zero-age main sequence for the ST distance and reddening scales. If such scales were adopted, then an entirely different interpretation of Figure 10 would be possible. Cannon (1970) and more recently Mermilliod (1981) have shown on an empirical basis that the mean absolute magnitude M_V of core-He-burning (CHeB) giants in the clump of open clusters is correlated with the age of the cluster for objects younger than 1 Gyr and near solar metallicities. Flower (1983) has put this relationship on a firm theoretical basis, and his results, for the metallicities adopted here, can be represented (Hardy *et al.* 1984) in the log age versus $M_V{}^F$ (the absolute magnitude of the faintest clump stars) plane as

$$\log t = 0.28\, M_V{}^F + 8.47\ . \qquad (3)$$

From inspection of Figures 9 and 10 the faintest "clump" stars would be at $M_V \approx +1$ [if indeed $(m-M)_{AV} = 19.3$)], corresponding to $t = 0.6$ Gyr. The "subclump" region would then be formed by a continuous population of horizontal branches (i.e., CHeB stars) of decreasing age (and increasing brightness) in which the most populous "clump" happens to be at $V = 19.3$, rather than exclusively a sequence of red giants populating the ascending subgiant branch. We are not able to test this hypothesis by looking at possible bright turnoffs along the main sequence due to the loss of contrast introduced by the presence of the populated very bright main sequence and the unknown degree of completeness for stars fainter than $V \sim 20$.

In the Galaxy such a sequence of "clumps" is clearly present in the young cluster system with the vertical section running upward from the Hyades locus to NGC 2281 through NGC 3532 and NGC 6475, as shown in Figure 1 of Mermilliod (1981). At $(m-M)_{AV} = 18.9$, on the other hand, the more populous clump at $V = 19.3$ is already near the faintest limit of the CHeB sequence (Flower 1983). The reader will notice that the previous argument would invalidate any *a priori* identification of a subgiant branch in Figure 10 which could then be used to set a distance independently of the main sequence. Indeed if one were to assume *a priori*, by analogy with the Galaxy, that the "clump" is at $M_V = +0.5$, then $(m-M)_{AV} = 18.8$![3]

Within the constraints imposed by the uncertainties described above, our preferred interpretation based upon the dV distance points toward the existence of an underlying very strong stellar population which is older than about 3 Gyr and on which is superposed a young population still undergoing formation. This younger population is typified by the observed main sequence and, very likely, by some of the red giants. The presence of very red bright red giants is reminiscent of an asymptotic giant branch (AGB) in the sense of Aaronson and Mould (1982) and is also suggestive of an intermediate-age population. Uncertainties in the AGB models coupled with serious discrepancies with other dating procedures (Hodge 1983) prevent us from using the information on the AGB in a more quantitative way.

The observed population appears to be older than the field population of the LMC bar (which may be representative of the disk as a whole), where the subgiant branch is largely unimportant when compared with the younger "clump" or with the red giant branch (Hardy *et al.* 1984). Stars of all ages including old globular cluster–like stars are represented in both systems, as RR Lyrae variables seem to be common occurrences (Graham 1972). The difference, mostly one of degree, seems to lie in the older median age of the SMC stellar disk. In this context it is important to recall the assertion (Stryker and Butcher 1981 and references therein) that a large-scale event triggered star formation in the LMC 2–4 Gyr ago. The case could be made from our data that such an event was proportionally more intense in the SMC, although further study to fainter magnitudes is clearly needed to firmly establish the relative importance of the ≤ 3 Gyr subgiant branch which we believe to be stronger in the SMC.

The question of the exact rate of star formation as a function of age, which is perhaps the most interesting from the standpoint of theories of galaxy formation and evolution, cannot be answered with our data. Given the resolution problems implicit in ground-based observations, it should be obvious that reaching and identifying the turnoff points corresponding to the *different* superposed epochs of star formation will have to wait for space-based observations. On the other hand, *imagery* performed in the light of physically defined narrow-band photometric systems such as the

[3] This argument, however, does not apply to the *C-M* diagram of K3 or L1 (Gascoigne, Bessell, and Norris 1981), where the absence of a bright main sequence unmistakably establishes the presence of a true subgiant branch. Notice that for the ST distance to be valid their horizontal branches will have to be excessively bright at $M_V = 0$.

DDO system could provide reliable masses—and hence ages (Hardy 1979 and references therein)—for hundreds of clump stars at bright ($V \approx 20$) magnitudes where confusion is less critical. Thanks to the new generation of linear detectors (CCD, photon-counting arrays) this approach may prove to be an alternative ground-based procedure capable of providing more reliable information on the rate of star formation in nearby galaxies than the less-sensitive classical *C-M* diagram.

E. H. wishes to thank the Director of the Mount Wilson and Las Campanas Observatories for the granting of observing privileges at Las Campanas. Likewise, E. H. acknowledges the hospitality of ESO/GENEVE and particularly the enthusiastic collaboration of Dr. J. Melnick in digitizing the data. D. D. is grateful to the Federal and Provincial Governments for the tenure of graduate Fellowships.

This investigation was supported by the National Science and Engineering Research Council of Canada.

REFERENCES

Aaronson, M., and Mould, J. 1982, *Ap. J. Suppl.*, **48**, 161.
Arp, H. 1958*a*, *A.J.*, **63**, 273.
———. 1958*b*, **63**, 487.
Bruck, M. T. 1978, *Astr. Ap.*, **68**, 181.
Bruck, M. T., and Hawkins, M. R. S. 1981, in *IAU Colloquium 68, Astrophysical Parameters for Globular Clusters*, ed. A. G. Davis, Philip and D. S. Hayes (Schenectady: L. Davis Press), p. 261.
Bruck, M. T., and Marsoglu, A. 1978, *Astr. Ap.*, **68**, 193.
Cannon, R. D. 1970, *M.N.R.A.S.*, **150**, 111.
de Vaucouleurs, G. 1978, *Ap. J.*, **223**, 730.
Durand, D. 1982, unpublished M.Sc. thesis, Université Laval.
Durand, D., Hardy, E., and Melnick, J. 1984, *Ap. J.*, submitted.
Flower, P. J. 1983, preprint.
Gascoigne, S. C. B., Bessell, M. S., and Norris, J. 1981, in *IAU Colloquium 68, Astrophysical Parameters for Globular Clusters*, ed. A. G. Davis Philip and D. S. Hayes (Schenectady: L. Davis Press), p. 223.
Graham, J. 1972, in *IAU Colloquium 21, Variable Stars in Globular Clusters*, ed. J. D. Fernie (Dordrecht:Reidel).
Hardy, E. 1979, *A.J.*, **83**, 319.
Hardy, E., Buonanno, R., Corsi, C. E., Janes, K. A., and Schommer, R. A. 1984, *Ap. J.*, **278**, in press.
Hodge, P. 1982, *Ap. J.*, **256**, 447.
———. 1983, *Ap. J.*, **264**, 470.
Kinahan, B. K., and Härm, R. 1975, *Ap. J.*, **200**, 330.
Maeder, A., and Mermilliod, J. C. 1981, *Astr. Ap.*, **93**, 136.
Mathewson, D. S., Ford, V. L., Schwarz, M. P., and Murray, J. D. 1979, in *IAU Symposium 84, The Large-Scale Characteristics of the Galaxy*, ed. W. B. Burton (Dordrecht: Reidel), p. 547.
Mermilliod, J.-C. 1981, *Astr. Ap. Suppl.*, **44**, 467.
McClure, R. D., Twarog, B. A., and Forrester, W. T. 1981, *Ap. J.*, **243**, 841.
Patenaude, M. 1978, *Astr. Ap.*, **66**, 225.
Rheault, C., and Hardy, E. 1980, in *Applications of Digital Image Processing to Astronomy, Proc. Soc. Photo-Opt. Instr. Eng.*, **264**, 200.
Sandage, A., and Tammann, G. A. 1974, *Ap. J.*, **190**, 525.
Stetson, P. B., and Harris, W. E. 1977, *A.J.*, **82**, 954.
Stryker, L. L., and Butcher, H. R. 1981, in *IAU Colloquium 68, Astrophysical Parameters for Globular Clusters*, ed. A. G. Davis Philip and D. S. Hayes (Schenectady: L. Davis Press), p. 255.
Walker, M. F. 1972, *M.N.R.A.S.*, **159**, 379.

DANIEL DURAND and EDUARDO HARDY: Département de Physique, Faculté des Sciences et de Génie, Université Laval, Québec, Canada G1K 7P4